AFRL-AFOSR-VA-TR-2019-0332

Aperiodic Silicon Photonics: Inverse Design, Fast Algorithms, and Fundamental Aspects

Shanhui Fan
LELAND STANFORD JUNIOR UNIVERSITY

03/07/2019
Final Report

DISTRIBUTION A: Distribution approved for public release.

Air Force Research Laboratory
AF Office Of Scientific Research (AFOSR)/ RTB1
Arlington, Virginia 22203
Air Force Materiel Command

REPORT DOCUMENTATION PAGE

Form Approved OMB No. 0704-0188

The public reporting burden for this collection of information is estimated to average 1 hour per response, including the time for reviewing instructions, searching existing data sources, gathering and maintaining the data needed, and completing and reviewing the collection of information. Send comments regarding this burden estimate or any other aspect of this collection of information, including suggestions for reducing the burden, to Department of Defense, Executive Services, Directorate (0704-0188). Respondents should be aware that notwithstanding any other provision of law, no person shall be subject to any penalty for failing to comply with a collection of information if it does not display a currently valid OMB control number.
PLEASE DO NOT RETURN YOUR FORM TO THE ABOVE ORGANIZATION.

1. REPORT DATE *(DD-MM-YYYY)*
08-11-2019

2. REPORT TYPE
Final Performance

3. DATES COVERED *(From - To)*
15 Aug 2015 to 14 Aug 2018

4. TITLE AND SUBTITLE
Aperiodic Silicon Photonics: Inverse Design, Fast Algorithms, and Fundamental Aspects

5a. CONTRACT NUMBER

5b. GRANT NUMBER
FA9550-15-1-0335

5c. PROGRAM ELEMENT NUMBER
61102F

6. AUTHOR(S)
Shanhui Fan, Jelena Vuckovic

5d. PROJECT NUMBER

5e. TASK NUMBER

5f. WORK UNIT NUMBER

7. PERFORMING ORGANIZATION NAME(S) AND ADDRESS(ES)
LELAND STANFORD JUNIOR UNIVERSITY
450 SERRA MALL
STANFORD, CA 94305-2004 US

8. PERFORMING ORGANIZATION REPORT NUMBER

9. SPONSORING/MONITORING AGENCY NAME(S) AND ADDRESS(ES)
AF Office of Scientific Research
875 N. Randolph St. Room 3112
Arlington, VA 22203

10. SPONSOR/MONITOR'S ACRONYM(S)
AFRL/AFOSR RTB1

11. SPONSOR/MONITOR'S REPORT NUMBER(S)
AFRL-AFOSR-VA-TR-2019-0332

12. DISTRIBUTION/AVAILABILITY STATEMENT
A DISTRIBUTION UNLIMITED: PB Public Release

13. SUPPLEMENTARY NOTES

14. ABSTRACT
The overall goal of the program is to push towards the ultimate limits for information density and energy per bit in on-chip information processing, through innovations in aperiodic silicon nanophotonic structures. Towards this goal we pursued experimental, computational, and theoretical explorations of aperiodic photonic structures.

15. SUBJECT TERMS
inverse design, aperiodic structures, optical devices, Aperiodic Silicon Photonics

16. SECURITY CLASSIFICATION OF: a. REPORT	b. ABSTRACT	c. THIS PAGE	17. LIMITATION OF ABSTRACT	18. NUMBER OF PAGES	19a. NAME OF RESPONSIBLE PERSON
Unclassified	Unclassified	Unclassified	UU		POMRENKE, GERNOT
					19b. TELEPHONE NUMBER *(Include area code)* 703-696-8426

Standard Form 298 (Rev. 8/98)
Prescribed by ANSI Std. Z39.18

AFOSR Project: Aperiodic Silicon Photonics: Inverse Design, Fast Algorithms, and Fundamentals

Final Report

I. Administrative Information

Grant Number: FA9550-15-1-0335
Project Start Date: 15 August 2015
Project End Date: 14 August 2018
PI: Shanhui Fan
Phone: 1-650-724-4759. Email: shanhui@stanford.edu
Spilker Room 314, Stanford University, Stanford, CA 94305
Co-PI: Jelena Vuckvic and David A. B. Miller, both from Stanford University
Program Manager: Dr. Gernot Pomrenke
Phone: (703) 696-8426. Email: gernot.pomrenke@afosr.af.mil

II. Program Objective

The overall goal of the program is to push towards the ultimate limits for information density and energy per bit in on-chip information processing, through innovations in aperiodic silicon nanophotonic structures. Increasing use of optics is essential both (i) to eliminate the dominating power dissipation in information processing, which is the charging and discharging of electrical interconnect lines and (ii) to continue to scale the density of information transfer at the chip scale by avoiding the scale-invariant capacity limitations of electrical wiring. Novel nanoscale optical technology is essential for exploiting the full channel density of optics at small scales and for enabling the continued scaling of active optical and optoelectronic devices into the attojoule range.

For a given information network, its capacity is directly related to the number of orthogonal channels available for information. The overall trend in optical communication has been to exploit as many orthogonal channels as possible. This has driven the development of Wavelength Division Multiplexing (WDM), Time Division Multiplexing (TDM), and more recently has led to the emergence of spatial mode division multiplexing.

For on-chip communication networks that are being rapidly developed for optical interconnect applications, with the chip bi-section bandwidth far exceeding Tbit/second and rapidly increasing, and with the constraint of a limited chip real estate, there is a critical need to pack information carrying channels and devices as densely as possible. Therefore the ability to use multiple spatial modes to carry information on-chip is a very attractive prospect.

Since all linear optical devices are mode converters, a key challenge then is to achieve arbitrary control of spatial modes, and moreover to do so in a foot print that is as small as possible. In this proposal, we describe several approaches to address this challenge. We will show that arbitrary mode conversion can always be designed in self-tuned manner, by cascading a number of Mach-Zehnder interferometers. We also show that more compact devices for modal manipulation can be realized by inverse design and fast optimization that creates aperiodic silicon photonic structures.

DISTRIBUTION A: Distribution approved for public release.

The ability to design aperiodic silicon photonic structures to meet performance objectives also points to new capability for achieving ultra-low power switching and modulation devices. We will specifically apply inverse design techniques towards developing structures with optimal performance in nonlinear information processing applications.

III. Scientific Approach

In this program we will pursue experimental, computational, and theoretical explorations of aperiodic photonic structures. Specifically, Vuckovic will pursue both computational and experimental work on inverse design of aperiodic silicon photonic structures. Fan will focus on developing fast algorithms that uncover the underlying physics of ensembles of aperiodic structures containing large numbers of member structures. The computational and experimental efforts here will be strongly coupled with the theoretical efforts by Miller on arbitrary modal conversion, and on theoretical limits of aperiodic photonic structures. These efforts in addition will benefit from ongoing collaborations with Professors Mark Brongersma's work in aperiodic plasmonics, and Professor Stephen Boyd's expertise in optimization theory and practice. We have on-going interactions/collaborations with AFRL and HP labs in related areas and the proposed efforts will further strengthen these interactions.

IV. Team Members

The PI's of our team are Professors Shanhui Fan, Jelena Vuckovic, and David Miller, all from Stanford University.

Graduate students supported by the grant: Alexander Piggott, Sacha Verweij

Other students who contributed to the grants: Jan Petykiewicz, Logan Su, Jerry Yu Shi

V. Major Accomplishments to Date

We have proposed efforts along the following three directions:

Thrust 1: Inverse design
Thrust 2: Fast algorithms for nanophotonic simulations
Thrust 3: Theory

We have made substantial progresses along each of the thrusts. In Thrust 1, Vukovic has computationally designed and experimentally demonstrated highly compact and efficient aperiodic structures for wavelength and mode splitting. Fan has carried out a large-scale search landscape analysis of an ensemble of photonic crystal structures to shed light on the performance of global search and optimization algorithm. In Thrust 2, Miller has developed a systematic algorithm for the design of "forward-only" optical structures with arbitrary performance characteristics. Fan has developed a multi-frequency finite-difference frequency-domain algorithm for simulations of active nanophotonic devices, and has further develop this method for study of on-chip acousto-optic interactions. In Thrust 3, Miller has developed a theoretical bound for the minimum size of optical components for a given optical functionality.

Below we provide more in-depth discussion on our scientific accomplishments:

Thrust 1: Inverse Design

- **Inverse Design Taking into Account Fabrication Constraints (Vuckovic)**

DISTRIBUTION A: Distribution approved for public release.

A major concern when designing devices with arbitrary topologies is ensuring that the devices are fabricable. In the case of nanophotonic devices, the main constraint is that the features must be large enough to be accurately resolved by the lithography system being used to fabricate the devices. To address this issue, we have directly incorporated heuristic fabrication constraints into our optimization algorithm. By allowing only large features, we can now design devices, which are compatible with industry-standard photolithography systems, which have considerably lower resolution than the specialized electron-beam lithography systems we currently use.

We choose a heuristic approach to applying fabrication constraints. We use curvature filtering to ensure that all features are greater than a characteristic size. All features with a radius of curvature smaller than a chosen threshold are smoothed out. Since curvature filtering, does not prevent the formation of narrow bridges and gaps, we also periodically search the design for bridges and gaps below a threshold width, and eliminate them. Mathematically, all these approaches are implemented using a level set method, which couples to the underlying electromagnetic modeling.

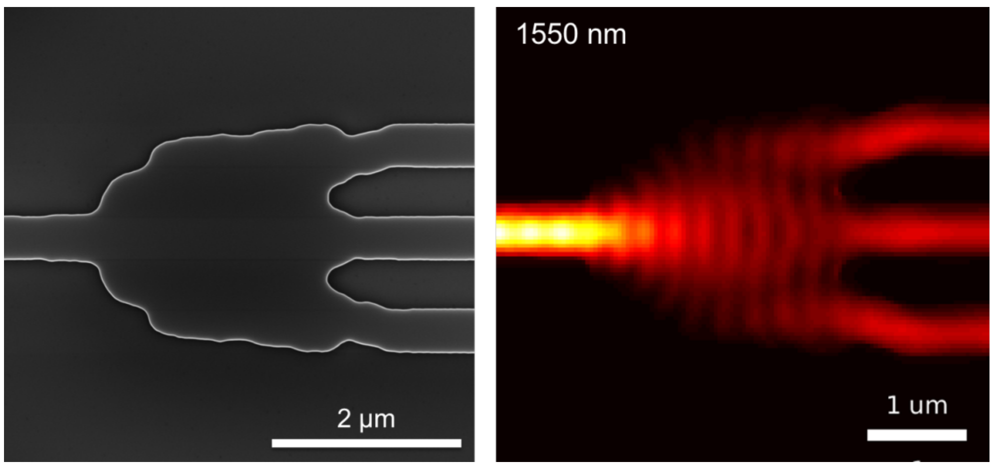

Figure 1: Broadband 3-way power splitter. Here, we have plotted a scanning-electron micrograph (SEM) of the fabricated device alongside the simulated electromagnetic energy density at 1550 nm.

We have designed a number of structures using our fabrication-constrained algorithm. We typically use a minimum feature size of 100 nm, which corresponds to the smallest hole we can reliably fabricate using our current fabrication process in the Stanford Nanofabrication Facility.

The first device we designed and fabricated is a broadband 3-way power splitter, illustrated in Figures 1 and 2. The device is designed to equally split power into three output waveguides with high efficiency over a broad wavelength range of 1400 – 1700nm. No device with comparable performance or size exists in the current literature. We also experimentally measured and characterized this device.

The second device is a 3-channel wavelength demultiplexer, illustrated in Figures 3 and 4. The output channels, centered at wavelengths of 1490, 1530, and 1570 nm, are more closely spaced than our previous device. The footprint, however, remains reasonably small, covering an area of approximately 5 x 6 μm, and is smaller than any previously demonstrated 3-way wavelength splitter. At the center wavelengths, the simulated insertion loss is approximately 1.5dB, and the simulated contrast is > 15dB.

The third device is a spatial mode demultiplexer that takes the TE_{10} and TE_{20} modes of a 750 nm wide input waveguide and routes them to the fundamental TE modes of two 400 nm wide output waveguides. The device has an average insertion loss of 0.826 dB and a contrast better than 16 dB over the design bandwidth of 1400-1700 nm.

DISTRIBUTION A: Distribution approved for public release.

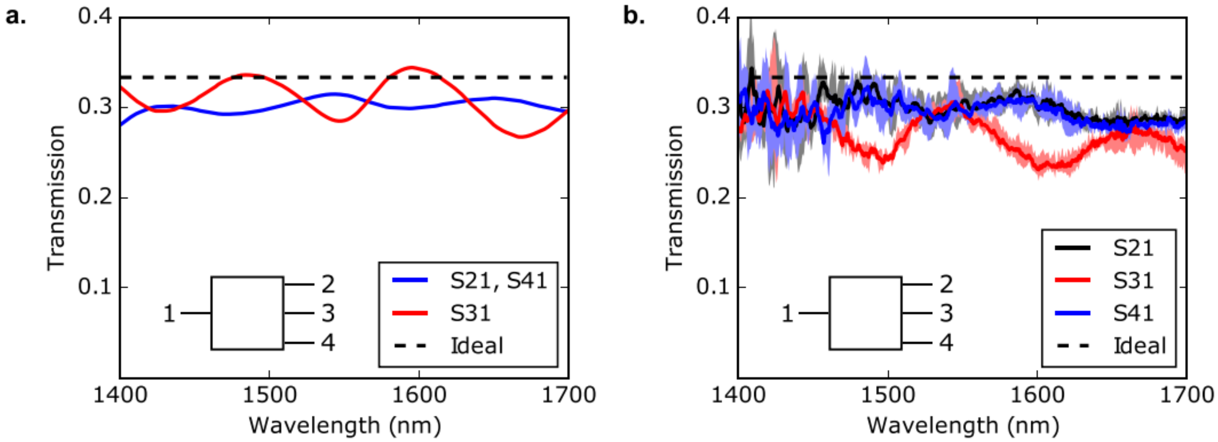

Figure 2: (a) Simulated transmission characteristics and (b) measured transmission characteristics of the broadband 3-way power splitter. The upper and lower output arms have exactly the same output power since the device is symmetric. The ideal output power of 1/3 per output arm is indicated with a dashed line.

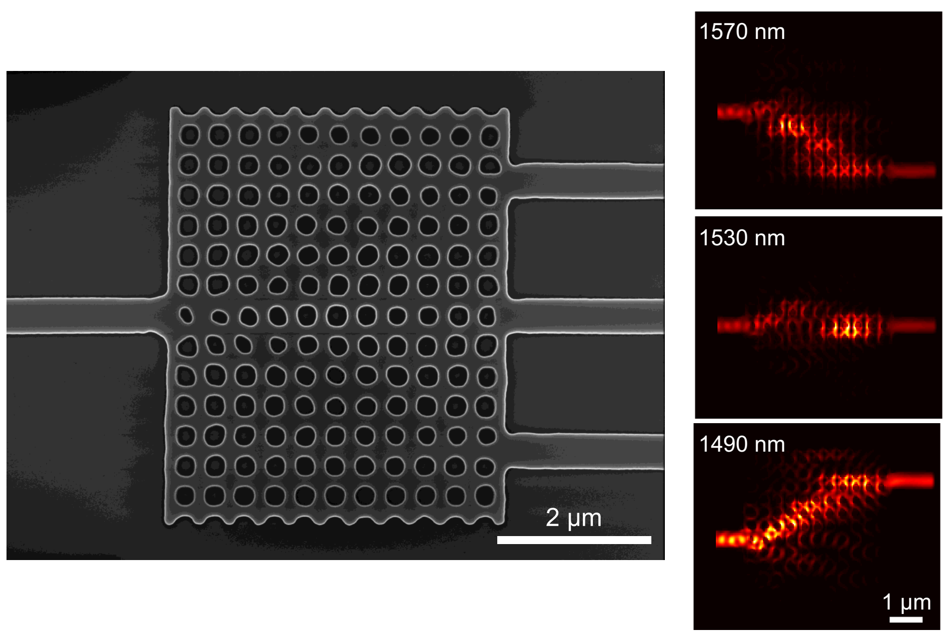

Figure 3: 3-channel narrowband wavelength demultiplexer. Here, we have plotted a scanning-electron micrograph (SEM) of the fabricated device alongside the simulated electromagnetic energy density at the design wavelengths of 1490, 1530, and 1570 nm. This particular device was designed by using a regular array of circular holes as a starting point.

DISTRIBUTION A: Distribution approved for public release.

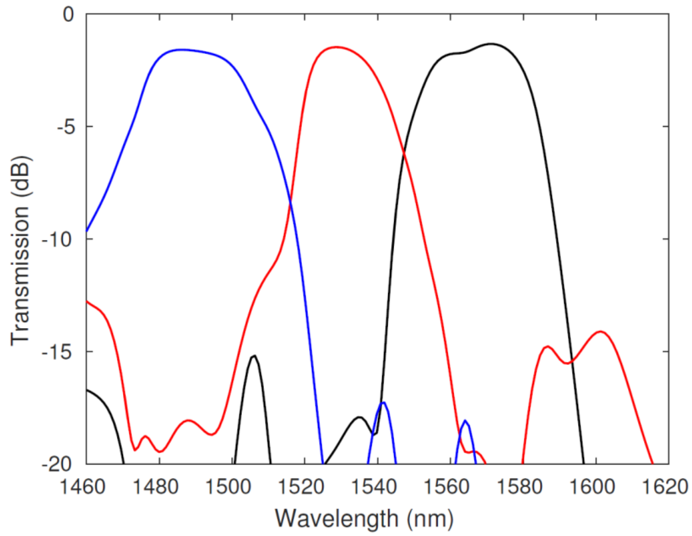

Figure 4: Simulated transmission characteristics of the 3-channel narrowband wavelength demultiplexer. The power in each output waveguide is indicated using different colours. The three passband channels are clearly visible.

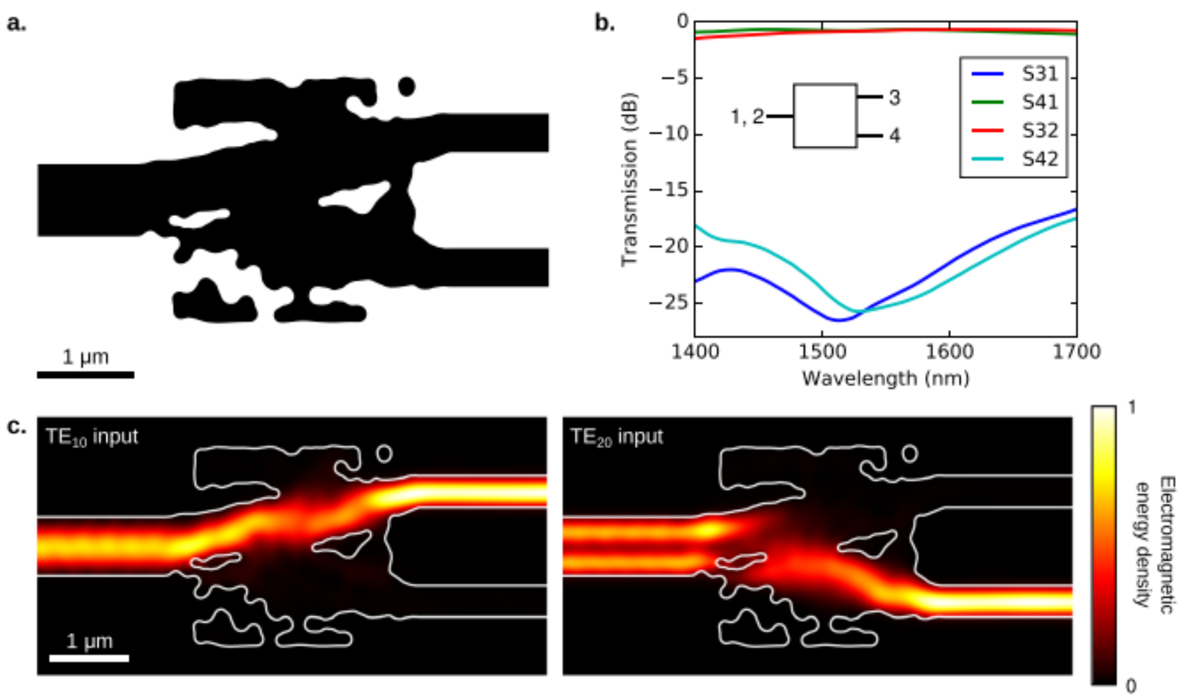

Figure 5: A spatial mode demultiplexer that takes the TE_{10} and TE_{20} modes of a 750 nm wide input waveguide and routes them to the TE_{10} mode of two 400 nm wide output waveguides. Here we present (a) the final design, (b) simulated S-parameters, and (c) the electromagnetic energy density at 1550 nm. The fields and S-parameters were calculated using finite-difference time-domain (FDTD) simulations.

- **Inverse Design of Narrowband Wavelength Demultiplexer (Vuckovic)**

In wavelength division multiplexing (WDM) schemes, splitters must be used to combine and separate different wavelengths. Conventional splitters are fairly large with footprints in hundreds

DISTRIBUTION A: Distribution approved for public release.

to thousands of square microns, and experimentally-demonstrated MMI-based and inverse-designed ultra-compact splitters operate with only two channels and large channel spacing (>100 nm).

In this project, we designed an efficient, narrowband, three-channel demultiplexer by augmenting our existing nanophotonic design algorithm with a technique we call biasing. Our design algorithm is split into two optimization stages. In the first stage, the permittivity is allowed to vary continuously between that of the cladding and that of the device. In the second stage, the permittivity is restricted to either the cladding or the device. By using biasing in the first stage, we were able to provide a better initial condition for the second stage.

We design a mere 24.75 μm^2 device with operating wavelengths at 1500 nm, 1540 nm, and 1580 nm. Unlike our previous photonic-crystal-based wavelength demultiplexer design, this design employs the continuous stage optimization technique to find a suitable starting point for discrete optimization, resulting in an entirely different type of structure. Consequently, the device is much more robust to fabrication than the photonic-crystal-based design. We verified our design by experimentally fabricating and characterizing the device. We measured an average peak insertion loss of -2.29 dB with under -10.7 dB crosstalk. The consistency of the measurements across four-identically fabricated devices demonstrates the fabrication insensitivity.

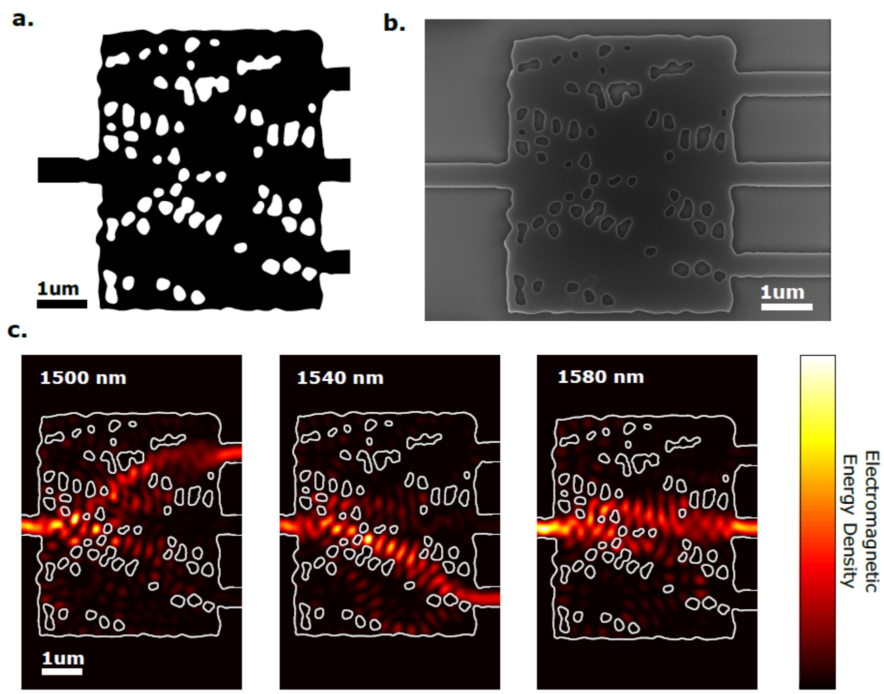

Figure 6: The three-way narrowband demultiplexer. (a) Design of the device. Black is silicon and white is silica. (b) SEM micrograph of the fabricated device. (c) Electromagnetic energy density at the operating wavelengths.

DISTRIBUTION A: Distribution approved for public release.

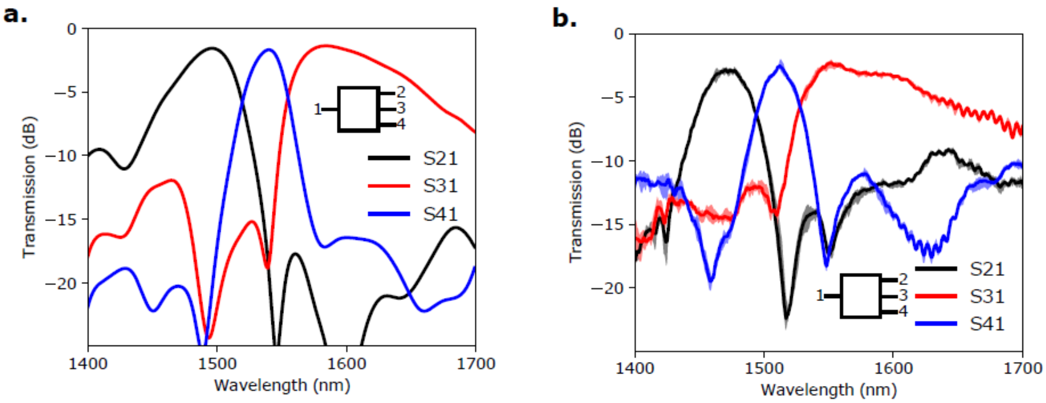

Figure 7: Simulated and measured S-parameters for the demultiplexer where S_{ij} is the transmission from port j to port i. (a) Simulated transmission calculated using the finite-difference time-domain (FDTD) method. (b) Measured transmission. Measurements from four identically-fabricated devices are overlaid on top of each other.

- **Inverse Design of Grating Couplers (Vuckovic)**

Because of their simplicity in both processing and alignment, grating couplers are an attractive way to couple light onto a chip. Despite the extensive literature on grating couplers, the grating design has typically been limited to either parameter sweeps or metaheuristic optimization methods, such as genetic algorithms and particle swarm optimization, which take a lot of time. In this project, we applied our inverse design approaches to develop an automated process to designing efficient grating couplers for different geometries and functionalities quickly and efficiently. Using this approach, we are able to demonstrate that blazed gratings are ideal for coupling light with near-unity efficiency.

Building on our existing work, our design process features three stages. First, the permittivity is parametrized continuously between that of the cladding and that of the device. Next, the permittivity distribution is converted to a discrete grating. Finally, the discrete device is further optimized with minimum feature size constraints.

The two key features of the design process are the generation of initial condition and the discretization process. First, unlike in previous works where the initial condition is physics-motivated and carefully-selected, the initial condition to our design process can be chosen uniformly at random. This enables us to explore a larger class of devices previously not explored by other design techniques. Moreover, this enables the optimization to work effectively for new geometries where the theory may not be very well developed. Second, the discretization process is an optimization problem itself that finds a good initial condition for the discrete process.

As an example, we present below two of the designs. The first is a wavelength-demultiplexing grating coupler where incident light at a wavelength of 1310 nm is coupled to the left waveguide and 1490 nm is coupled to the right waveguide. The second is a blazed grating waveguide that has a simulated coupling loss of under 0.17 dB.

DISTRIBUTION A: Distribution approved for public release.

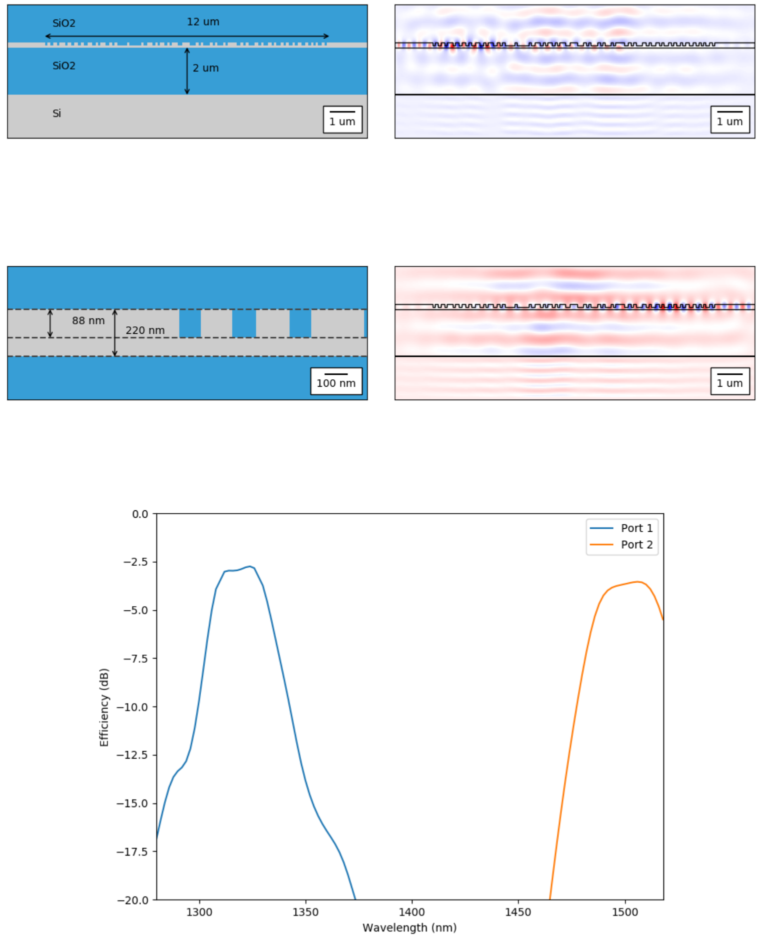

Figure 8: Design of wavelength-demultiplexing grating coupler. 1310 nm light is coupled to the left (port 1), and 1490 nm light is coupled to the right (port 2). Blue is silica and gray is silicon. The feature sizes exceed 100 nm.

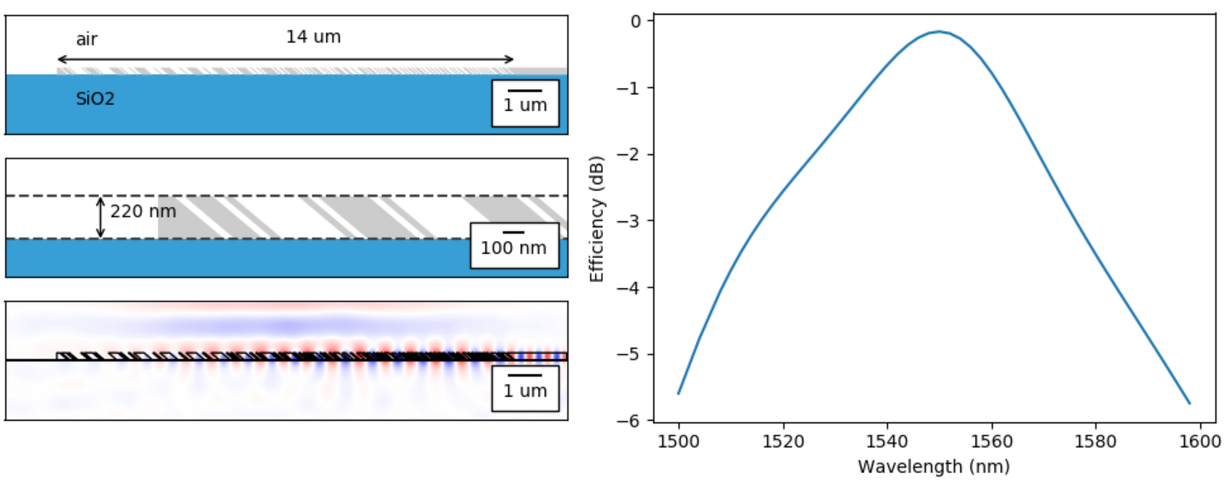

Figure 9: Design of 0.17 dB loss blazed grating coupler. Blue is silica, white is air, and gray is silicon. The coupler design has features larger than 50 nm and requires a 50 degree etch.

DISTRIBUTION A: Distribution approved for public release.

- **Search Landscape Analysis For Nanophotonic Design (Fan)**

Systematic design optimization of optical structures is opening new and advancing existing frontiers in the control of light, from ultra-compact wavelength- and mode-division multiplexing to performance enhancement of energy conversion. To exploit systematic design optimization's full potential in optics, search algorithms capable of efficiently sifting large design spaces are critical.

The degree to which a search algorithm exploits problem structure determines its efficacy. Thus, in the methodical analysis that is often key to understanding, and improving, search behavior, analysis of problem structure --- or search landscape analysis --- is a crucial component. Despite this, search landscape analysis is largely absent from the otherwise rapidly growing literature on search algorithms for design optimization of optical structures.

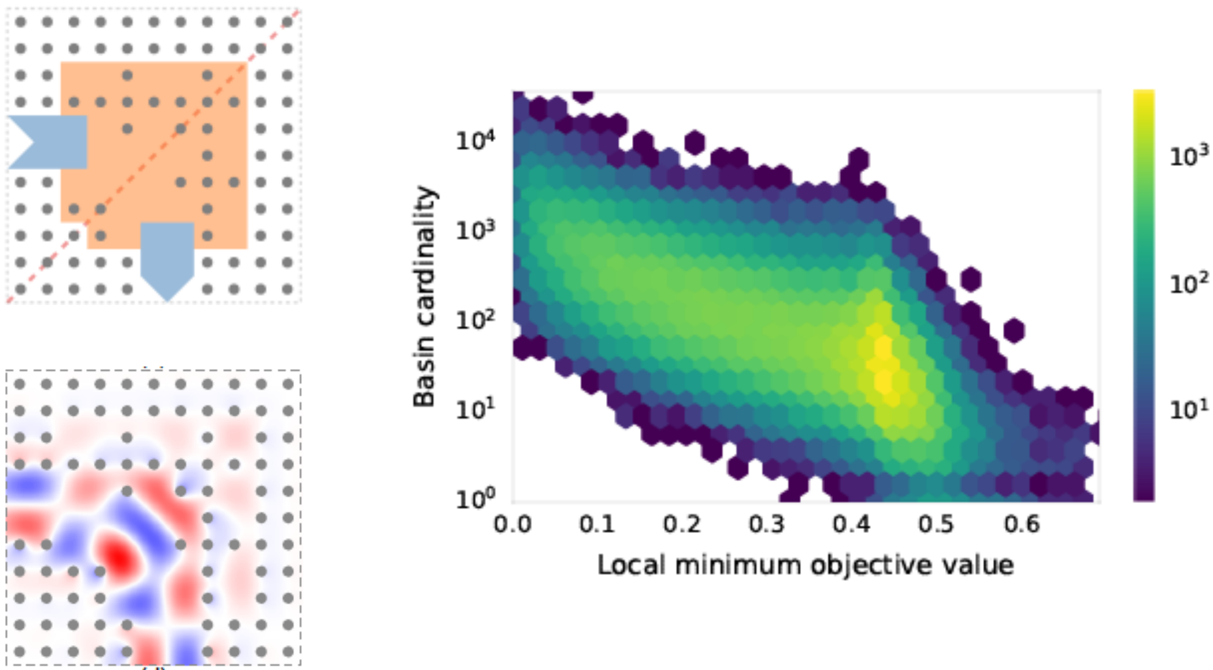

Figure 10: Search landscape analysis for design optimization of a multi-spatial-mode photonic crystal waveguide bend. (Left Panels) Example structures from the search space, altogether containing thirty-three million such candidate structures. (Right Panel) One analysis over all local optima in the search landscape. Plotted here is the size of the attraction basin (basin cardinality) against the performance (objective value) of each local optimum. Lower objective values imply better performance. Remarkably, the best performing local optima tend to have much larger attraction basins, which facilitates the performance of some classes of global search algorithms.

In this project, we illustrate how search landscape analysis can provide insight into search behavior in design optimization of optical structures. To this end, we consider design optimization of a photonic crystal waveguide bend that achieves high modal-content-preserving transmission (Figure 10). The design process involves searching a space containing thirty-three million candidate structures. Using fast numerical algorithms, we calculate the optical characteristics of all such thirty-three million candidate structures, and statistically analyze the results. That analysis reveals that the search landscape has substantial structure, which can be exploited to improve search algorithms. For example, we show that a relatively simple global optimization algorithm, namely restarted iterative best improvement, performs very well for this class of problems due to

DISTRIBUTION A: Distribution approved for public release.

some of the search landscape features uncovered in the preceding analysis. While we consider only a specific example, many of the search landscape features revealed can be related to general properties of the underlying physics, yielding insight into search landscape structure applicable to a broad class of optical design problems.

- **Objective-trait-bias Metaheuristics for Nanophotonic Design (Fan)**

This project builds upon the insights developed in the project above. The degree to which a search algorithm exploits problem structure determines its efficacy. Physically derived design optimization problems often contain rich structure that one can reason about on the basis of physical intuition; as evidenced in the above project, design optimization problems in optics are no exception. General-purpose search algorithms exploit little if any of this rich structure and thereby fail to achieve optimal performance on design optimization problems in optics. Augmenting such search algorithms with mechanisms that exploit this rich structure can significantly improve search efficacy.

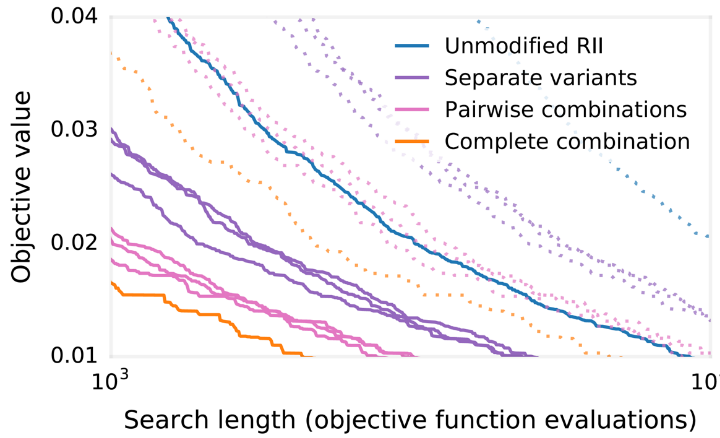

Figure 11: Performance comparison of the baseline search algorithm in blue (restarted iterative best improvement), variants improved via the objective-trait-bias metaheuristic described in this project in purple, and various hybrids of those variants in pink and orange. Solid lines reflect typical case search behavior, whereas dashed lines indicate near-worst-case search behavior.

Broadly applicable, physically motivated guiding principles for augmenting such search algorithms for design optimization problems in optics could substantially advance the field. The following objective-trait-bias metaheuristic exemplifies such guiding principles: design objectives often involve some set of traits --- necessary but insufficient conditions for performance. Examples include transmission or reflection, strong or weak absorption, broad or narrow bandwidth, modal conversion or preservation, or satisfaction or violation of symmetries. Now consider searching a design space for structures satisfying a design objective. Biasing the search toward design space regions that exhibit the requisite traits, and thereby more likely satisfy the design objective, should improve search performance.

In this project we illustrate how one might apply such guiding principles as well as their potential value. A case study, in which applying a concrete realization of the above metaheuristic leads to significantly better performing variants of a simple global search algorithm on a challenging design optimization problem, provides this illustration. The case consists of design optimization of a multi-spatial-mode photonic crystal waveguide bend as in the above project (Figure 10). Applying an instance of the above metaheuristic --- a transmission-bias metaheuristic --- leads to substantially improved variants of the simple global search algorithm discussed in the above project (Figure 11).

DISTRIBUTION A: Distribution approved for public release.

Thrust 2: Fast Algorithms For Ensemble Simulations

- **Universal "ReLLIM" design algorithm for "forward-only" optics (Miller)**

Optical components can usefully be divided into two categories:

(i) "forward-only" – in this category, the light in the optical system is never reflected backwards. Conventional optical lens systems, networks of Mach-Zehnder interferometers that do not "loop back", and even systems containing ring resonators can be like this.

(ii) "multiple scattering" – in this category, light from "later" or further into the structure can be reflected back to "earlier" parts of the structure. These could include complex scattering structures, photonic-crystal-like structures, and structures containing Fabry-Perot resonators.

The "multiple scattering" structures, as far as we understand them, are almost certainly likely to require "global" iterative design techniques; we can perform those designs, of course, these designs can be particularly compact and functional, and these are an important part of our work in this larger project.

For the "forward-only" structures, however, it is possible that we may be able to design them and set them up completely progressively, from the "earlier" parts through to the "later" parts, without having to go back and readjust or redesign the "earlier" parts once we have designed or set the "later" parts. Indeed, we have previously devised such progressive algorithms for particular architectures using meshes of Mach-Zehnder interferometers. These algorithms with those architectures are so simple that they can even be used in self-configuring manners, designing themselves based on specific inputs without any calculations. Extensions of these algorithms allow us to set the whole complex optical network up even without calibrating its elements and even compensating for some imperfections in the fabrication.

Though we had previously found these design and setup algorithms for specific, and very useful, architectures, it was by no means clear more arbitrary architectures could be set up progressively. Indeed, there are important classes of Mach-Zehnder mesh architectures for which there was no known progressive method to set them up.

Specifically, many interesting linear optical networks, such as lattice filters and a wide range of other possible systems based on meshes of interferometers, are difficult to fabricate with sufficient precision and cannot be configured progressively even using our previous setup algorithms. Now we have shown a new algorithmic approach that allows a broad category of optical networks to be set up in a progressive fashion, including correcting for fabrication imprecision. The approach works by progressively nulling interference locally in the network based on inputs calculated by considering the network operated in reverse; as a result, we have named this the "reversed local light interference method" (ReLLIM). Calibration is only required for the network inputs, not for components inside the network. With this approach we can show explicitly that we can set up lattice filters and rectangular meshes of interferometers, and we expect the approach can be applied to any such "forward-only" structure. Such an approach may increase the range of optical networks that can be mass-fabricated at reduced tolerances and corrected and set up in the field.

- **Multi-Frequency Finite-Difference Frequency-Domain Techniques for Active Nanophotonic Device Simulations (Fan)**

In recent years, there have been very significant interests in designing active nanophotonic devices. For instance, there are extensive works with electro-optical modulators for on-chip optical interconnects. Such modulators have in addition been used in the construction of optical isolators

DISTRIBUTION A: Distribution approved for public release.

and nonreciprocal metasurfaces, as well as in the realization of photonic topological effects. In designing such active devices, it is crucial to be able to accurately simulate their performances from the first principles of Maxwell's equations.

Nevertheless, direct simulation of active devices with traditional time-domain methods have been prohibitively expensive due to the inherently large time-scale difference between optical and modulation frequencies. While in optical communication devices the carrier frequency is at 200THz, the typically modulation frequency is on the order of 10's GHz. Consequently, a single modulation period corresponds to 10^5 optical cycles. Due to this constraint, many previous active device performances are only simulated approximately, and these simulations make approximations that inevitably neglect portions of the underlying device physics. In order to accurately and realistically simulate from first-principles these active devices, there is therefore an urgent need to develop a computational algorithm to efficiently perform multiple time-scale simulations.

To overcome this challenge, we formulated a multi-frequency finite-difference frequency-domain (MF-FDFD) algorithm in order to efficiently perform first-principles calculations of active devices that possess multiple time-scales. In the frequency domain, the physics of active devices can be rigorously formulated in terms of interactions between waves at different frequencies. By setting up frequency-domain simulations simultaneously at different frequencies and by allowing the interactions between wave components at these frequencies, one can formulate the steady-state response of a modulated system from an excitation source as a system of linear equations that can be solved self-consistently. Using this general and powerful technique, one can directly simulate a large class of active devices without the limitation in time-domain simulations as imposed by the existence of vastly differing time scales inherent in these problems.

We verify the performance of the MF-FDFD algorithm by demonstrating modal conversion in a waveguide structure with harmonically modulated permittivity. When computing the modal conversion between the even and odd modes of a modulated waveguide, we observe excellent agreement between the solutions from the MF-FDFD algorithm and coupled mode theory, which provides validation for our algorithm. Furthermore, the MF-FDFD algorithm reveals the effects of backward coupling, which is an underlying physics that is typically neglected in coupled mode theory treatments.

Having validated the performance of MF-FDFD, we demonstrate the application of the MF-FDFD algorithm to a realistic ring modulator structure, as shown in Fig. 12(a). At a wavelength of $\lambda = 1564.55$ nm, an input wave is critically coupled with the ring, resulting in zero transmission [Fig. 12(b)]. When we apply a small harmonic permittivity modulation at gigahertz in the ring waveguide, the sideband frequencies from the ring can couple from the ring to the waveguide, resulting in nonzero transmission. In Fig. 12(c), we show the coupling from the ring to the waveguide at the first sideband frequency. In Fig. 12(d), the transmitted power is plotted in time, and the power follows the waveform of the sinusoidal modulation.

In summary, we have formulated the MF-FDFD algorithm that can accurately perform first-principles simulations where there exists a large time scale difference. Using this general technique, we demonstrate that one can accurately and efficiently simulate devices that have frequency components with arbitrarily large discrepancies in their time scales.

DISTRIBUTION A: Distribution approved for public release.

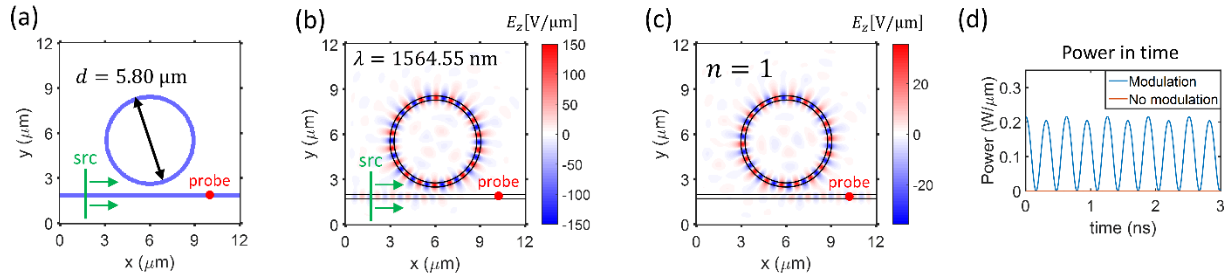

Figure 12: (a) Schematic of the ring waveguide modulator. (b) At λ=1564.55 nm, an input wave is critically coupled with the ring, resulting in zero transmission. (c) Plot of power at the first sideband frequency that couples out of the ring resonator when the ring is modulated. (d) Plot of the transmitted power in time. The transmitted wave follows the waveform of the modulation.

- **Acousto-optic Finite-Difference Frequency-Domain Techniques for On-chip Acousto-optic Device Simulations (Fan)**

Recently, there have been increasing interests in acousto-optic devices to harness photon-phonon interactions, most prominently through the process of the Stimulated Brillouin Scattering (SBS). Thus far, acousto-optic devices have been designed for many important micro- and nano-photonic structures for acousto-optic modulation, creation of lasers with ultra-narrow linewidths, frequency-comb generation, slow light applications, and on-chip signal processing devices.

Given the wide range of devices that can harness acousto-optic interactions, it is important to develop a general numerical technique that can facilitate the device design process. However, direct simulations of these devices face an intrinsic challenge that arises from the enormous time-scale difference between optical and acoustic waves, effectively rendering tradition time-domain simulation methods intractable. For instance, a typical optical wave has a frequency of around 200 THz, whereas acoustic waves usually have frequencies of around 5 to 10 GHz. Thus, even though in principle, one could simulate acousto-optic interactions with a standard first-principles time-domain simulation technique such as the finite-difference time-domain (FDTD) algorithm, a single acoustic wave cycle corresponds to around 10^5 optical wave cycles, or around 10^7 time steps. Thus, accurately treating photon-phonon interactions in time-domain simulations becomes prohibitively numerically expensive, and researchers typically adopt a modal-expansion technique to describe acousto-optic interactions from perturbation principles, which is difficult for complex geometries that support many modes. In order to accurately and realistically perform first-principle simulations of a general class of acousto-optic devices, there is an urgent need to develop a computational algorithm to efficiently and exactly simulate the interactions between optical and acoustic waves.

To overcome the numerical challenges and to enable first-principle calculations of photon-phonon interactions, we introduce an acousto-optic finite-difference frequency-domain (FDFD) technique for the simulation of acousto-optic devices. In the frequency domain, the physics of the acousto-optic system can be rigorously formulated as a system of coupled nonlinear equations, whose solution provides the steady-state dynamics of the acousto-optic systems. With such a frequency-domain solver, we bypass the need to compute field values at every time step, and can therefore directly simulate a general class of acousto-optic devices without the limitations in time-domain simulations as imposed by the vastly differing time scales between optical and acoustic waves.

Using the acousto-optic FDFD algorithm, we can perform a number of numerical simulations for acousto-optic devices. We first validate the acousto-optic FDFD algorithm by simulating the SBS phenomenon in a straight waveguide and compare its solutions with that of coupled mode theory,

DISTRIBUTION A: Distribution approved for public release.

and we observed excellent agreements between the two solutions. Furthermore, we showed that the acousto-optic FDFD method can capture the photon-phonon interactions at high powers, where coupled mode theory fails because of the breakdown of the slowly-varying envelope approximation.

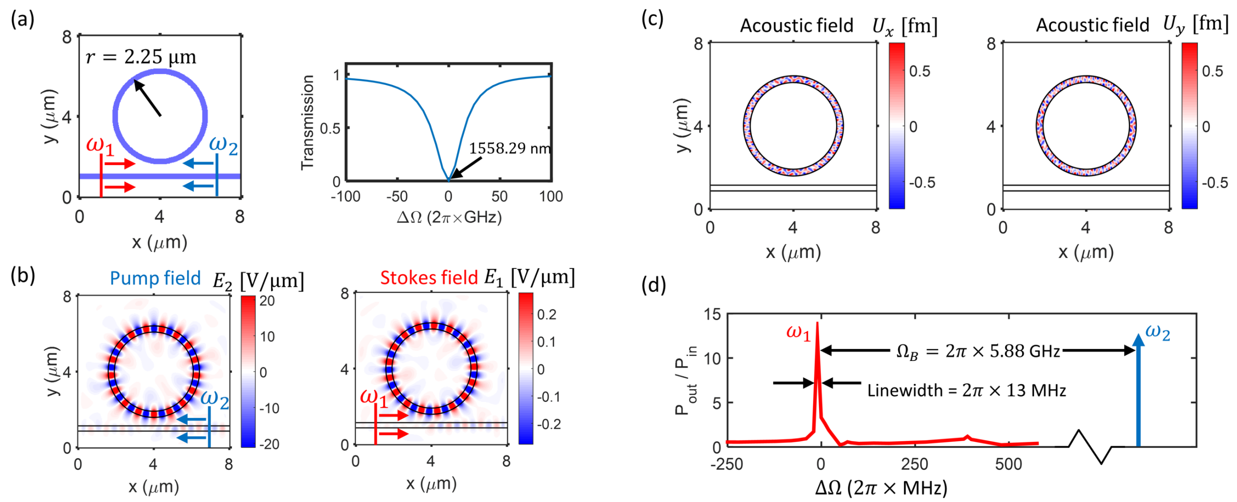

Figure 13: (a) Schematic of the acousto-optic ring waveguide and its spectrum. At λ=1558.29 nm, an input wave is critically coupled with the ring, resulting in zero transmission. (b) Field profiles of the forward Stokes wave and backward pump wave. When we counter-propagate a pump at $\boldsymbol{\omega_2}$ and a Stokes wave at $\boldsymbol{\omega_1}$ that are detuned by the SBS resonance frequency $\boldsymbol{\Omega_B = 2\pi \times 5.88}$ GHz, the Stokes wave is largely amplified as it propagates through the waveguide. (c) The acoustic field profile inside the ring. These complex patterns suggest that the ring is highly modal for acoustic waves. (d) Plot of the gain spectrum for the Stokes wave at different frequencies while keeping the pump frequency the same. This captures the ultra-narrow linewidth of the SBS process.

With the validation above, we can simulate a realistic on-chip acousto-optic device as shown in Fig. 13(a). The structure consists of an external straight waveguide coupled to a ring resonator, whose resonance frequency corresponds to an input wavelength of $\lambda = 1558.29$ nm. Near its resonance frequency, in the acousto-optic FDFD simulation, we counter-propagate a low-power Stokes wave at frequency ω_1 and a higher-power pump wave at frequency ω_2 that is detuned by the acoustic SBS frequency of the ring resonator, Ω_B, such that $\omega_2 - \omega_1 = \Omega_B$. In this setup, a resonant SBS process is excited inside the ring resonator, where optical and acoustic filed interact coherently through a stimulated process. Through this interaction, as can be seen from the field plots in Fig. 13(b), the Stokes wave is largely amplified as it travels outside the ring resonator. Furthermore, in Fig. 13(c), we plot the acoustic displacement field profiles inside the ring, whose complexity suggests that the ring resonator is highly multi-modal. Such complex modes is difficult to be captured using coupled mode theory but can be effectively simulated using the acousto-optic FDFD algorithm. Lastly, in Fig. 13(d), we fix the pump frequency at ω_2 and sweep the Stokes frequency ω_1 to capture the SBS process's gain spectrum. As is typical of SBS, the gain spectrum shows an ultra-narrow resonance of only 13 MHz. Such a narrow linewidth would be difficult to be captured using a traditional time-domain method, but our acousto-optic FDFD algorithm can efficiently simulate it because it bypasses the limitations imposed by the time-scale difference between optics and acoustics waves.

In summary, we have formulated an efficient way of simulating photon-phonon interactions from first principle. We hope to use this algorithm in the future for the design of acousto-optic devices, especially micro- and nano-scale devices that have complex geometries.

DISTRIBUTION A: Distribution approved for public release.

- **Domain-decomposition approach for fast simulation of nanophotonic devices (Fan)**

Nanophotonic structures often consist of large collections of repeated meta-atoms as in, for example, many functional photonic crystals or metamaterials. Furthermore, the individual meta-atoms often contain fine, subwavelength features that makes simulating large collections of these meta-atoms challenging. In simulating these structures, finding a way to exploit the high degree of repeated structure could provide significant efficiency improvements.

A simple and natural way to exploit the repetition of meta-atoms in such structures is to use a non-overlapping domain decomposition approach, for example a Schur complement domain decomposition. Domain decomposition has been investigated for nanophotonics extensively in the context of finite element methods using sophisticated iterative substructuring techniques, for example in finite element tearing and interconnect (FETI) methods [13, 16]. Additionally, variations focusing on solution of scattering problems using surface integral methods have also been studied. However, given the simplicity of finite difference methods relative to finite element methods, investigating simple domain decomposition methods for the former is worthwhile.

In this work we develop the Schur complement decomposition approach in finite-difference frequency-domain algorithms (Fig. 14). We show that the use of such an approach can drastically improve the convergence speed for iterative finite-difference frequency-domain method. (Fig. 14c). Such an improvement is important for the application of finite-difference frequency-domain method for photonic device optimization.

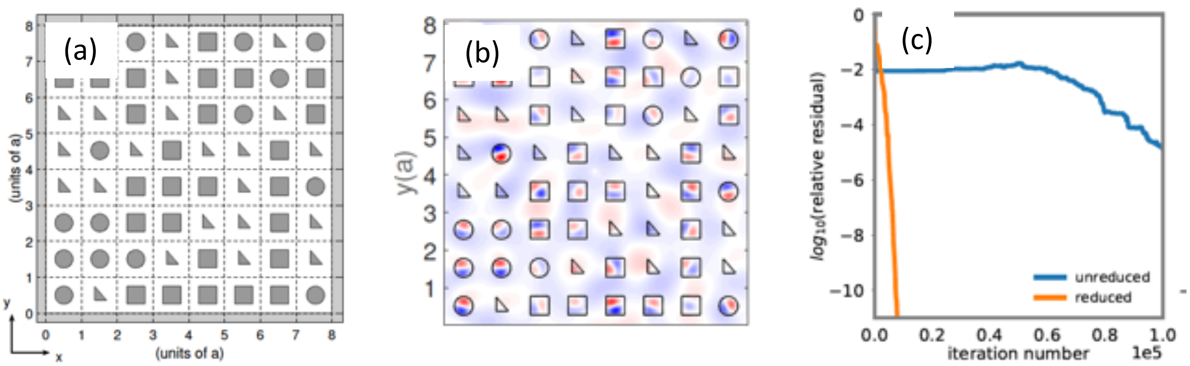

Figure 14: (a) Setup for Schur complement approach in finite-difference frequency-domain (FDFD) schemes. With Schur complement the linear system involves only coupling on the edge of the unit cells as indicated by the dashed lines. (b) The electric field for the structure shown in (a). (c) Comparison in convergence speed with the standard FDFD approach (blue curve), and with Schur complement. (orange curve). The use of the Schur complement leads to orders-of-magnitude improvement of the convergence speed.

Thrust 3: Theory

- **Minimum size for an optical component (Miller)**

Given the growing ability to perform arbitrary design of complex and compact optical elements, such as nanophotonic mode converters, it is increasingly important to know if there is a minimum size for such components. At the very least, that could tell us what size of volume of material to use to design a device.

Now we have first results suggesting a simple minimum size requirement for an optical component. This bound tells us the maximum number of independent channels or modes we can

DISTRIBUTION A: Distribution approved for public release.

control with a device if the device is to be efficient. If the device is to be reasonably universal among these channels, this limit does not otherwise depend much on what we want to do with the channel or mode. The number of channels M_C we can control grows linearly with the square of the maximum relative change in dielectric constant, and with the square of the minimum bounding dimension σ (in half-wavelengths) of the device volume. It depends only weakly on the specific shape of the device volume. For sheet-like objects (such as planar integrated optics), it grows only logarithmically with the size of the sheet. Specifically, then, this preliminary result is suggesting that

$$M_c \leq \mu_S \eta_{max}^2 \sigma^2$$

where η_{max} is the largest available relative change in dielectric constant in the structure, and μ_S is an overall "shape factor" that is ~ 1 for volumes like spheres and cubes, and grows only at best logarithmically as other dimensions are increased. This shape factor generally depends only weakly on shape. In upcoming work, we will be considering and cross-checking the implications of this preliminary result.

- **Universal radiation laws for all thermal emitters (Miller, Fan)**

So that objects can come to the same temperature just by exchanging electromagnetic radiation, radiation laws must relate the fraction of incident radiation absorbed by an object and the amount of radiation emitted when it is hot. Such laws are both fundamentally important and set limits to practical applications such as converting light to electricity and in heat and thermal management generally. Kirchhoff derived the key radiation laws that have been used now for some 150 years. However, these were derived using simplified models.

Specifically, diffraction was neglected, which means those laws are not necessarily reliable or meaningful for the modern situations where we routinely work with nanostructures much smaller than a wavelength, and where we our optics may be focusing to diffraction limited spots.

The original derivation also specifically presumed that the materials were all reciprocal; that might seem a small omission because non-reciprocal optics is very much the exception rather than the rule; the classic example is a Faraday isolator, which is an optical component that is relatively hard to make because it requires special materials and magnetic fields. However, the fundamental limit of solar energy conversion would appear to require the use of non-reciprocal materials, and so understanding radiation laws for such materials is of some fundamental importance.

We have derived new versions of radiation laws that avoid these problems, and discovered additional and unexpected radiation laws that substantially expand the fundamental relations between optical absorption and emission. In particular, we have obtained four new radiation laws. All of these fully include the effects of diffraction, and so are valid for small objects and for arbitrarily tight focusing. Three are valid for reciprocal and non-reciprocal optics, and one particularly broad one applies for all reciprocal optics.

The proofs exploit two novel approaches. First, we express all fields in terms of the mode-converter basis sets of beams; these sets, which can be uniquely established for any linear optical object, give orthogonal input beams that are coupled one-by-one to orthogonal output beams. The idea of expressing optics in terms of such sets explicitly comes out of our previous work on universal optical components. Second, we consider thought experiments using universal linear optical machines that we also proposed in our recent work; these machines allow us to couple appropriate beams and black bodies. This approach allowed us to derive a new core "first" law, valid for all optical systems, which states that the absorptivity of any mode-converter input beam is equal to the emissivity into the corresponding mode-converter output beam. This is unlike any previous radiation law. This law might seem rather restrictive because it only seems to apply to these specific beams, but note that it includes diffraction and works for non-reciprocal as well as reciprocal systems. We can use it to derive two broader laws that also apply to reciprocal and non-reciprocal systems; our "second" law gives unexpected equivalences of absorptivity and emissivity for broad classes of beams, and our "third" law is the full generalization of Kirchhoff's original law – essentially that the total absorptivity of an object is equal to its total emissivity. Finally, we are able to find a "fourth" law, which is perhaps one that people thought existed all along, but in fact was not proved. This one, which applies only to reciprocal systems, states that the absorptivity of any beam is equal to the emissivity into the "backwards" version of that beam; this law fully includes diffraction and so is valid also for small objects and for tightly focused beams, which the previous "directional" version of Kirchhoff's law actually was not.

As a final point here, these laws show an unexpected fundamental meaning to the "mode-converter" beams for any object: the mode-converter input beams are the ones with the maximum absorptivities, and the mode-converter output beams are the ones with the maximum emissivities.

- **Non-reciprocal geometric phase in nonlinear frequency conversion (Fan, in collaboration with Australian National University)**

In a collaboration with Professor Dragomir Neshev's group at the Australian National University, we describe analytically and numerically the geometric phase arising from nonlinear frequency conversion and show that such a phase can be made non-reciprocal by momentum-dependent photonic transition. Such nonreciprocity is immune to the shortcomings imposed by dynamic reciprocity in Kerr and Kerr-like devices. We propose a simple and practical implementation, requiring only a single waveguide and one pump, while the geometric phase is controllable by the pump and promises robustness against fabrication errors.

VI. Publications

2015

1. Alexander Y. Piggott, Jesse Lu, Konstantinos G. Lagoudakis, Jan Petykiewicz, Thomas M. Babinec, and Jelena Vučković, "Inverse design and demonstration of a compact and broadband on-chip wavelength demultiplexer," *Nature Photonics* 9, 374–377 (2015)

2016

2. Alexander Y. Piggott, Jesse Lu, and Jelena Vučković, "**Silicon Photonics: Design approach to integrated photonics explores entire space of fabricable devices**," *Laser Focus World*, 52 (3) (2016) (*Review*)

3. S. Verweij, and S. Fan, "Understanding search behavior via search landscape analysis in design optimization of optical structures", *Journal of the Optical Society of America B* 33, 2457 (2016).

4. Y. Shi, W. Shin and S. Fan, "A multi-frequency finite-difference frequency-domain algorithm for active nanophotonic device simulations", *Optica* 3, 1256 (2016)

DISTRIBUTION A: Distribution approved for public release.

2017

5. D. A. B. Miller, L. Zhu, and S. Fan, "Universal modal radiation laws for all thermal emitters," *Proceedings of the National Academy of Sciences*, **114**, no. 17, 4336-4341 (2017) doi:10.1073/pnas.1701606114.

6. Alexander Y. Piggott, Jan Petykiewicz, Logan Su & Jelena Vučković ".Fabrication-constrained nanophotonic inverse design," *Scientific Reports* 7, 1786 (2017).

7. Logan Su, Alex Y. Piggott, Neil V. Sapra, Jan Petykiewicz, and Jelena Vuckovic, "Inverse design and demonstration of a compact on-chip narrowband three-channel wavelength demultiplexer," under review in *ACS Photonics* (2017).

8. S. Verweij and S. Fan, "Objective-trait-bias metaheuristics for design optimization of optical structures," *Journal of the Optical Society of America B* 34, 1551 (2017).

9. Y. Shi, A. Cerjan, and S. Fan, "Acousto-optic finite-difference frequency-domain algorithm for first-principles simulations of on-chip acousto-optic devices", *APL Photonics* 2, 020801 (2017).

10. K. Wang, Y. Shi, A. S. Solntsev, S. Fan, A. A. Sukhorukov and D. N. Neshev, "Non-reciprocal geometric phase in nonlinear frequency conversion", Optics Letters 42, 1990 (2017).

11. D. A. B. Miller, "Setting up meshes of interferometers – reversed local light interference method," Optics Express 25, 29233-29248 (2017).

2018

12. N. Zhao, S. Verweij, W. Shin, and S. Fan, "Accelerating convergence of an iterative solution of finite difference frequency domain problems via schur complement domain decomposition," Optics Express 26, 16925–16939 (2018).

13. S. Verweij and S. Fan, "Impact of objective bandwidth and frequency sampling density on search landscape structure and search performance in design optimization of optical structures," Journal of Optics 20, 115002 (2018).

14. Sean Molesky, Zin Lin, Alexander Y. Piggott, Weiliang Jin, Jelena Vučković, Alejandro W. Rodriguez. Nature Photonics 12, 659–670 (2018)

15. Logan Su, Rahul Trivedi, Neil V. Sapra, Alexander Y. Piggott, Dries Vercruysse, Jelena Vučković, "Fully-automated optimization of grating couplers", Optics Express 26, 4023-4034 (2018).

16. Logan Su, Alexander Y. Piggott, Neil V. Sapra, Jan Petykiewicz, and Jelena Vučković, "Inverse Design and Demonstration of a Compact on-Chip Narrowband Three-Channel Wavelength Demultiplexer", ACS Photonics 5, pp. 301–305 (2018)

VII. Honors and Awards Since 2015

- **Jelena Vuckovic:** APS Fellow; OSA Fellow; IEEE Fellow, Plenary talks at CLEO 2016, NSFO15 conference in Troyes, and at the DATE conference in Dresden.
- **Shanhui Fan:** Thomson Reuters Highly Cited Researcher in Physics, since 2015; Vannevar Bush Faculty Fellowship from the Department of Defense, 2017; Plenary talk at the SPIE Photonics West 2017, Nature Conference on Nanophotonics and Integrated Photonics 2018.

DISTRIBUTION A: Distribution approved for public release.

VIII. Issues of Concerns

None.

DISTRIBUTION A: Distribution approved for public release.